

Technical Article

The Methods of Quasicrystals Producing

H. Bakhtiari^{1,*}, M. Abaei¹, M. R. Rahimpour¹, M. Farvizi¹, M. J. Eshraghi¹¹Materials and Energy Research Center, Karaj, Iran.

Received: 22 February 2021- Accepted: 02 June 2021

Abstract

Quasicrystals are structures that are both regular and non-periodic. In quasicrystals, there is an iterative rule in the arrangement of atoms, along with abnormal rotational symmetry for crystals, that is, they form patterns that fill space but have no transfer symmetry. These structures are generally made of alloys of aluminum, copper, nickel, magnesium, zinc, zirconium, and titanium. These materials have attracted the attention of many researchers in recent years due to their extraordinary physical and mechanical properties. Due to the extraordinary properties and different production methods, it can be expected that these materials will be used more in different industries in the near future. Therefore, it is very important to study the methods of preparation of these materials. In this article, we first introduce the quasicrystals and their outstanding properties and then examine their common production methods, which include melt spinning, mechanical alloying, coating method, sputtering, physical vapor deposition, and thermal spraying, along with their advantages and disadvantages.

Keywords: Quasicrystal, Properties, Production Methods.

1. Introduction

Quasicrystals are considered to be a subset of crystalline materials that have a discrete diffraction pattern and are found in a large set of materials. Generally, such materials are described as having a long-range periodic order without translational symmetry [1-3]. Most commonly, these materials can display 'unusual' orders of rotational symmetry, where unusual is considered an order of symmetry which is incommensurate with periodic or Bravais lattice systems (for example, 5-fold, 10-fold, 12-fold). Intermetallic alloys exhibiting these structural properties are the most abundant and most studied quasicrystalline systems, and are called 'quasicrystals' (QCs), derived and shortened from 'quasi-periodic crystals' [4-5]. In 1984, while experimenting with a fast-frozen manganese-aluminum alloy, Daniel Schachtman was confronted with a structure that he could neither assume to be crystal nor to consider as an amorphous material. The structure observed by Schachtman had an icosahedral phase with axes of rotational symmetry of types 3 and 5. However, there is no degree of rotation symmetry of type 5 in, degree 1 of crystals. In conventional crystallography, a crystal has a rotational symmetry property in which, lattice maps onto itself after rotation through the angle $2\pi/n$; it is mathematically proven in solid state physics text books that $n = 1, 2, 3, 4,$ and 6 are the only allowed values, whereas $n = 5$ or $n > 6$ are forbidden

symmetries for crystals [7]. This can be demonstrated using a triangle or hexagon (also square, rectangle, diamond, and oblique) tile as a unit cell. As shown in (Fig. 1.a), one can tile a plane without any overlapping and creating any gaps and build a lattice in which all unit cells are identical and have the same surroundings. However, such a lattice or complete tiling cannot be obtained using unit cells or tiles with forbidden symmetries such as pentagons, heptagons, octagons, and decagons (Fig. 1.b) [8]. As mentioned, quasicrystals have many potential and actual applications in applied sciences and research, and it is even possible to reach nanostructures. Important methods for the production of these materials include melting, physical vapor deposition, mechanical alloys, thermal spraying techniques, plasma firing and atomization [9-10].

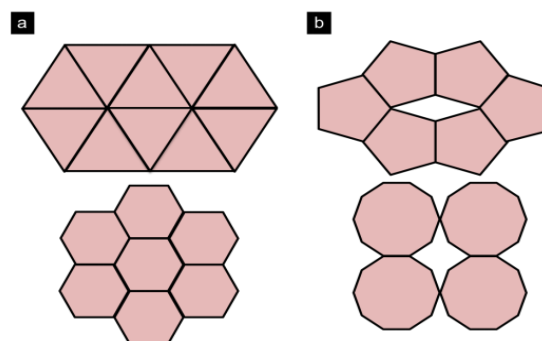


Fig. 1. (a) Allowed rotational symmetries, (b) disallowed rotational symmetries in conventional crystallography [8].

*Corresponding author

Email address: hamid.bakhtiari60@gmail.com

Given the above, some of the most common methods of producing quasi-crystals and the characteristics of these methods have been investigated in this study.

2. Classification of Quasicrystal

QCs systems can be studied and identified based on Al, Mg, Zn, Cd, Ti, Zr and Hf, some of which are mentioned below [11]:

Mg-based: Mg-Zn-Al, Mg-Al-Cu/Ag/Au, Mg-Al-Zn-Cu, Mg-Al-Pd, Mg-Cd-Yb

Al-based: Al-Mn/Cr/Fe, Al-Mn-Si/Ge, Al-Cu-(Fe, Ru, Os), Al-Pd-(Mn, Re), Al-Pd-(Os, Ru)

Ti-Zr-based: Ti-Cr/Ni/Zr, Ti-Zr-Ni

Cu-based: Cu-Ga-Mg-Sc

Ag-In-based: Ag-In-Yb, Ag-In-Mg-Yb, Ag-In-Ca, Ag-In-Mg-Ca

Zn-based: Zn-Mg-Sc, Zn-Mg-RE (RE = Y and Gd, Tb, Dy, Ho, Er)

Cd-based: Cd-Mg-RE (RE = Y and Nd, Sm, Tb, Dy, Ho, Er, Tm, Lu), Cd-Mg-Yb, Cd-Mg-Ca, Cd-Ca, Cd-Yb

3. Outstanding Properties in Quasicrystals

The properties of quasicrystals due to their unique atomic structure can include extraordinary items such as good hardness, high corrosion resistance, low coefficient of friction, high thermal and electrical insulation, and high surface energy. Due to the mentioned properties, these alloys are suitable for applications such as anti-wear coatings, non-viscous coatings, food industry, thermal insulation coatings, corrosion-resistant coatings, medical industry, reinforcements for polymer and metal composites, hydrogen storage, and etc. [12-15].

4. Methods of Producing Quasicrystals

4.1. Melt Spinning

Several methods have been used to determine the quasicrystal shapes. The first quasi-crystalline phases were variable and were obtained during rapid solidification. The mentioned method is like producing metallic glasses with cooling speed of 10^5 to 10^9 Ks⁻¹ to prevent the formation of high temperature equilibrium phases. There are several techniques that permit varying the rate of supercooling at the nucleation state, such as melt spinning or planar flow casting. In these processes, molten alloys are squirted onto a rotating wheel (Fig. 2). The liquid, when dropped on the wheel, is quenched at a rate of the order of 10^6 Ks⁻¹ and the sample is obtained as ribbons a few μm thick and a few mm wide. The quenching rate can be changed to some extent by varying the rotation speed of the wheel. The ribbons generally contain single grains

of quasicrystal with sizes of about $1 \mu\text{m}$ across. To improve the physical structure and mechanical properties of the resulting filaments, they are often transferred directly to the stretching process. The big advantage of melt spinning is that it does not need to be filtered, as no solvent is used. Another advantage is its very high production speed, which varies from a few hundred meters per minute to several thousand meters per minute [16].

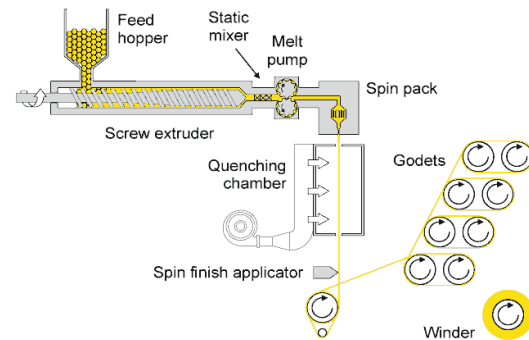


Fig. 2. Schematic view of a melt spinning apparatus [16].

The recent progress in rapid solidification processing (RSP) of crystalline alloys has allowed a degree of microstructural control that has never been achieved before by any conventional ingot metallurgy methods. These attributes of RS have been utilized in many alloy systems in designing alloys that exhibit principally improved mechanical properties [16-18].

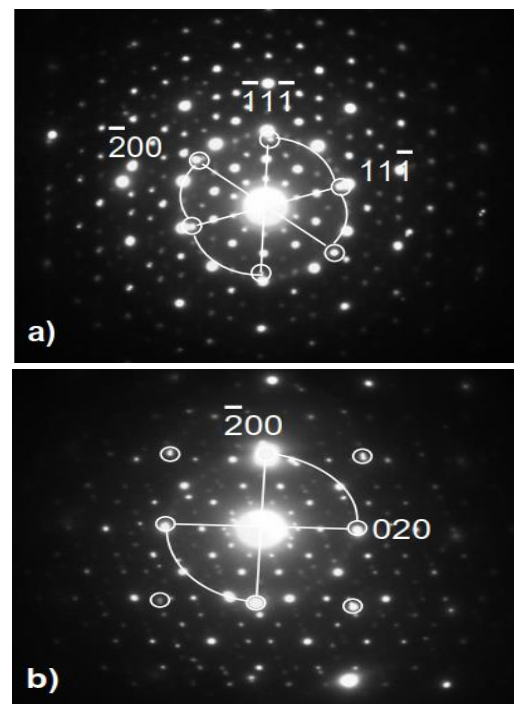


Fig. 3. Selected area electron diffraction patterns showing five-fold rational symmetry visible in (a) $[011]\alpha$ and (b) $[001]\alpha$ orientation [20].

Table 1. Quasicrystalline alloys fabricated by casting method [16].

Metallic System	Alloy	Processing route	Phases
Al-Cu-Fe-Cr	$Al_{65}Cu_{22}Fe_{10}Cr_3$	Melt-spinning 1 mm plate – Cu quenched	i-QC + d-Qc
	$Al_{67}Cu_{20}Fe_5Cr_8$	Arc-melting+annealing at 600°C Melt-spinning	i-QC + d-QC + τ -AlCu(Fe) d-QC + τ -AlCu(Fe) d-QC + τ -AlCu(Fe)
Al-Cu-Fe-Ni	$Al_{63}Cu_{18}Fe_{10}Ni_3$	Melt-spinning	i-QC + 2 B2 cubic phases + λ - $Al_{13}Fe_4$
	$Al_{64}Cu_{20}Fe_{13}Ni_9$	Melt-spinning	i-QC + 2 B2 cubic phases
Al-Ni-Co-Cr	$Al_{72}Ni_{19}Co_7Cr_2$	Melt-spinning	d-QC + d-QC(Cr-rich) + $Al_3Ni(Co)$
	$Al_{72}Ni_{20}Co_5Cr_3$	Melt-spinning	$Al_3Ni_2(Co)$ d-QC + d-QC(Cr-rich) + $Al_3Ni(Co)$ $Al_3Ni_2(Co)$
Al-Ni-Co-Cu	$Al_{71}Ni_{20}Co_7Cr_2$	Melt-spinning	d-QC + $Al_3Ni(Co)$ $Al_3Ni_2(Co)$
	$Al_{70}Ni_{20}Co_5Cr_5$	Melt-spinning	d-QC + $Al_3Ni(Co)$ $Al_3Ni_2(Co)$

These solidification conditions make it possible to make composites by conventional casting. Due to the well-known quasicrystalline compounds, future applications could lead to the discovery of crystal-based aluminum-based composites[17]. Table. 1. gives the metal systems, alloys, and four-phase aluminum phases performed by the casting method .Školáková et al [19]. In the study of Al-Cu-Fe, Al-Cu-Fe-Ni, Al-Cu-Fe-Cr alloys by melt spinning and hot extrusion showed that the structure of cast alloys is completely heterogeneous and mainly from Aluminum background formed when needle-like intermetallic phases such as $Al_{13}Fe_4$, $CuAl_2$ appeared. Katarzyna Stan [20]. Examination of Al-Mn-Fe showed that crystalline crystals in the form of dendrites, spherical particles and quasi-like structure can be observed.

The cross-sectional area of the ribbon at high cooling rate showed microstructure leading to particles smaller than icosahedral (200-250 nm) embedded in the aluminum matrix. Large quasi-crystalline dendrites were seen outside. Higher hardness was also obtained for the area with smaller particle size. Although the quasi-crystalline particles became rich in manganese and iron, the composition was somewhat different and eutectic. It was found that the axes are 5 times parallel to the axes of type $\langle 011 \rangle$ and $\langle 001 \rangle$ of (Al) (Fig. 3.) and the quasi-perturbation constant was determined to be 4.61%. These results have been confirmed by other researchers for quasi-crystals containing aluminum and manganese as key elements. Zupanic et al. [21] also achieved the following results in the production of quasicrystal by this method: Melted ribbons are composed of quasicrystalline particles 40 to 60m thick. The quasi-crystalline phase structure was basic in Al-Mn-Be icosahedral alloys. Beryllium and manganese were enriched in semi-crystalline particles. The particles, however, contained significant amounts of Be (~35 in%). The results showed that the rate of quasicrystalline formation of Al-Mn alloys containing beryllium depends on its presence in the quasi-crystalline phase [21]. Their results showed that excellent mechanical properties at ambient temperature and high creep resistance

high temperatures can be attributed to the high thermal stability of phase i, the proper distribution of phase i for alloys containing Y along the grain boundary and the role of solid solution reinforcement [21].

4.2. Mechanical Alloying

Mechanical alloying is a powder production technology that uses a powder mixture of primary elements to produce homogeneous materials. In this process, the powder mixture is subjected to high energy collisions inside a mill. These collisions can produce supersaturated solid solutions, semi-stable crystal phases, nanostructures, amorphous materials, metal powders, nanocomposite powders, nanopowders, and metal-ceramic composites. Mechanical alloying is suitable for achieving phases that are in the narrow range of components and stable at low temperatures. Mechanical alloying expands the combined range (phase-field) of the phases and makes the preparation of the quasicrystal phase more technically interesting and attractive[22]. All reactions occur in the solid-state: The advantage of this is that the complex solidification behavior problems encountered in conventional casting can be overcome. Mechanical alloying is also very suitable for the production of composite materials. In this case, on the one hand, a very precise mixture of components is obtained and on the other hand, it preserves the unique properties of the materials in the final product [22]. So far, alloys such as $Al_{65}Cu_{23}Fe_{12}$, $Al_{65}Cu_{20}Fe_{15}$, $Al_{70}Cu_{20}Fe_{10}$ have been obtained from the Al-Cu-Fe quasi-crystalline base composition by mechanical alloying. Pseudocrystals are often unstable and may change to crystalline or amorphous form if milled for a long time. Excessive distortions in the structure of quasicrystals make it difficult to synthesize these materials directly through mechanical alloying; Their formation is strongly influenced by the composition of the raw materials of the elements, milling time, heat treatment, and other parameters. Therefore, the use of subsequent heat treatment methods to achieve this structure is recommended.

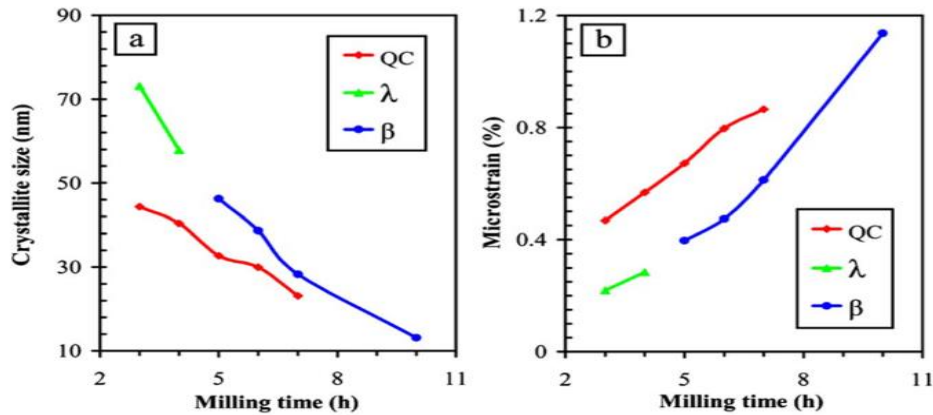


Fig. 4. (a) Crystallite size and (b) microstrain of the $\text{Al}_{67}\text{Cu}_{20}\text{Fe}_{10}\text{B}_3$ alloy versus milling time after 3 h of the MA process [23].

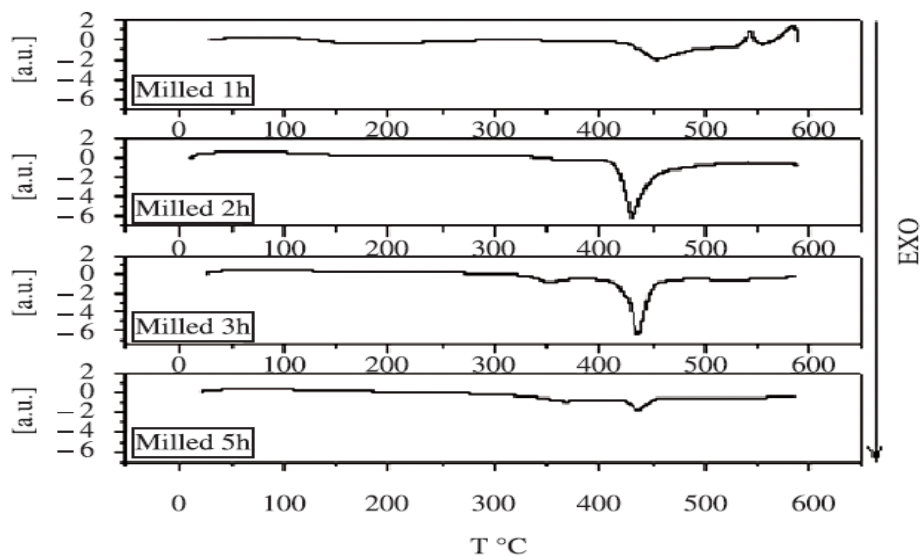


Fig. 5. DSC results obtained for the powders milled for different times [25].

The fact that heat treatment is an effective method for forming a quasicrystal phase is agreed upon by many researchers, some of which are mentioned below.

Production of $\text{Al}_{59}\text{Cu}_{25.5}\text{Fe}_{12.5}\text{B}_3$ pseudocrystalline nanocrystals by mechanical alloying was investigated by Amini et al. [23]. According to the results, stable icosahedral phase can be formed using high energy planetary mills, milling for 4 hours mainly leads to form a single-phase Crystal. The stability of the quasicrystalline phase is about 300 $^{\circ}\text{C}$, which is unstable at higher temperatures and leads to the formation of crystalline phases and reduced volume fraction of the quasicrystalline phase.

However, if the annealing operation is performed at the appropriate temperature after the milling process, a quasicrystalline phase is formed next to the crystalline phases. The microhardness of the milled powders at about 4 hours, when the quasicrystalline phase is predominant, is about 10.73 GPa. Fig. 4. shows the crystallite size and microstrain variation for crystalline and quasicrystalline phases with milling times. It is seen that

the crystallite size of the respective phases is in the nanometric scale. Also, the correlation of lattice and microstrain parameters with the milling time is estimated [23].

The structural evaluation of $\text{Al}_{62.5}\text{Cu}_{25}\text{Fe}_{12.5}$ icosahedral single-phase quasicrystal with different grain sizes in the nano range during heating showed that the recrystallization peaks of nanocrystalline nanocrystals are sharply displayed to reduce the quasi lattice strain and an increase in grain size is attributed.

The results of this researcher show that CTE for quasicrystals increases with decreasing grain size [24]. In the Al-Cu-Fe compound, a mixture of aluminum, copper, and iron powders with an atomic ratio of 15-20-65% was obtained by high-energy milling method. DSC analysis of milled powders showed that phase changes occur during heating in the temperature range of 440 $^{\circ}\text{C}$ (Fig. 5). Phase changes indicate that annealing after high-energy milling increases the probability of forming a pseudo-crystalline ψ phase. Details show that an

exothermic peak of about 150 °C was observed in the milled powders for 1 h. This courier disappeared after 2 hours of milling for long milling times [25].

4.3. Coating Method

4.3.1 Sputtering

The sputtering method, as one of the coating methods, has different stages including evaporation of the source material, transfer of steam from the source to the substrate, and the formation of a thin layer on the substrate [26]. Types of sputtering devices include: magnetic sputtering, parallel diode sputtering, flat diode sputtering, triode sputtering, magnetron sputtering. One of the most important advantages of the sputtering method is that many materials that can not be produced during a chemical process or require high heat for thermal evaporation can be layered with the sputtering method. Another advantage of the sputtering process is that it can be used for many materials. Controlling the thickness of the layers is very simple in the sputtering method. Spraying can be done on large surface targets and eliminate the problem of non-uniform layer thickness. It is very easy to clean the substrate by ion bombardment in this way. It is possible to provide coatings free of any porosity. Another advantage of sputtering is the preservation of the stoichiometry of the constituent elements of various materials and the thin film of refractory materials. In the sputtering method, the surface of the layer is also bombarded by energetic ions and is therefore damaged. There are two approaches to reducing the impact of negative ions and reducing their effects: one is the use of high gas pressure to reduce the energy of negative ions by repeated collisions with atoms and ions in the plasma environment, and the other is off-axis sputtering in which the substrate, it is not in the direction of the target and its special design reduces the number of negative ions colliding with the layer and thus reduces surface damage and defects. Magnetron sputtering is performed under vacuum and can be used to create crystal-like coatings on polymers, metals and ceramics. [27].

Fig. 6. shows the sputtering schematic with three and four targets. The angle of the sputtering gun was kept at 30° according to the normal of the substrate. The distance from the bed to the target was 18 cm. The slope of the material composition was controlled by the sputtering ability applied to the targets and according to the evaluation of the amount of sediment by the quartz crystal thickness monitor. Base pressure below 10⁻⁶ and working pressure at 0.3 Pa with argon gas were considered [28]. Studies have been performed to make Al-Cu-Fe and Al-Cu-Fe-Cr alloys by magnetron co-sputtering. Table. 2. summarizes the sputtering and annealing coatings at different Al-Cu-Fe temperatures.

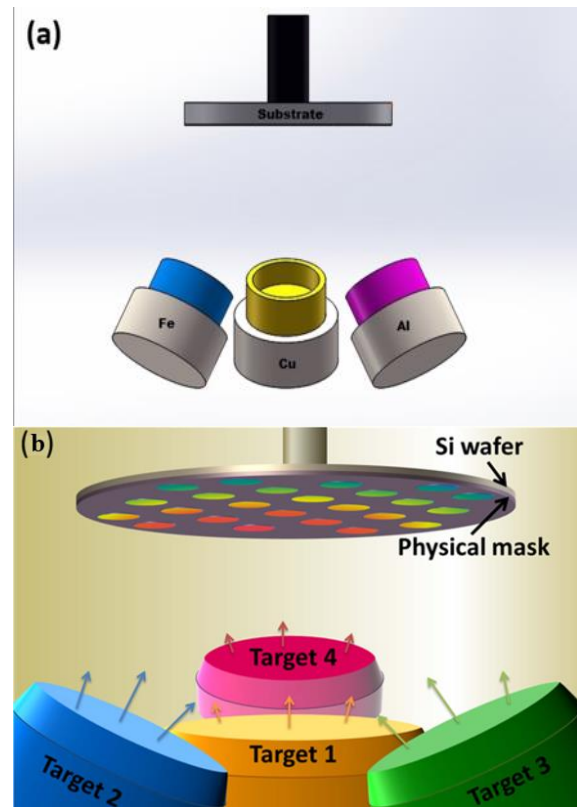


Fig. 6. Schematic diagram showing the co-sputtering deposition a) three targets b) four targets [28].

Table. 2. Brief of the reported phase stability in Al-Cu-Fe sputtered and annealed at different temperatures [29].

% at.	Substrate Cooling	Thickness	As-sputtered	400 °C	450 °C	550 °C	600 °C	750 °C	850 °C
Al ₆₅ Cu ₂₀ Fe ₁₅	N ₂ liquid	10 μm	Amorphous	—	Cubic P.	—	QC	—	—
Al ₆₅ Cu ₂₀ Fe ₁₅	N ₂ liquid	10 μm	Amorphous	—	Cubic P.	—	QC	—	—
Al ₆₄ Cu ₂₃ Fe ₁₃	—	150–200 nm	NanoCrys	Cubic P.+I	—	—	—	—	—
Al ₆₀ Cu ₂₂ Fe ₁₀ O ₈	—	10 μm	Amorphous/ NanoCrys	—	Approxim ant R	—	—	—	QC
Al ₆₁ Cu ₂₅ Fe ₁₀ B ₄	—	5 μm	Amorphous/ NanoCrys	—	—	—	QC P.+ Cubic	—	—
Al ₆₂ Cu _{25.5} Fe _{12.5}	—	100 nm	Amorphous/ NanoCrys	Amorphous /NanoCrys	NanoCrys P. +α-Al +Cubic	—	QC P.+ Cubic	—	—

Table 3. Synthesis of structural and morphological details of samples with thick layers [26].

Sample Composition	Preparation technique Thickness (μm)	Substrate temperature (K)	Post-treatment Temperature (K) Time (h)	Structure Morphology Size of grain
TiNiZr-0 $\text{Ti}_{41.5}\text{Ni}_{17}\text{Zr}_{41.5}$	PLD 0.6	548	None	Icosahedral Textured Columnar. 50 nm (width)
TiNiZr-1 $\text{Ti}_{41.5}\text{Ni}_{17}\text{Zr}_{41.5}$	PLD 0.6	298	None	Icosahedral nanocrystalline 2 nm
AlCuFe-0 $\text{Al}_{62.5}\text{Cu}_{25}\text{Fe}_{12.5}$	Reactive magnetron Sputtering 6	298	673 2	Icosahedral nanocrystalline 3 nm
AlCuFe-1 $\text{Al}_{62.5}\text{Cu}_{25}\text{Fe}_{12.5}$	Reactive magnetron Sputtering 6	298	None	Amorphous - -

Table 4. Nanohardness and elastic modulus of as-sputtered and annealed Al-Cu-Fe films [27].

as-sputtered Annealed					
		200°C	400°C	550°C	750°C
Hardness (Gpa)	9.44	10.16	11.29	13.49	14.75
E (Gpa)	114.4	123.0	132.2	141.4	150.7

Brien et al. [26] Showed the following results in bulk samples with high-thickness films by laser deposition, sintering of powder from crushed ingots or atomized powder, and dispersion. The alloys were compared with different conditions (deposition method, heat treatment and substrate temperature) and the results showed that $\text{Al}_{62.5}\text{Cu}_{25}\text{Fe}_{12.5}$ nanostructured isodoxyl dernel with a grain size of 3 nm was obtained (table 3). The hardness results of the dispersed films deposited by the maximum load (30 mN) of fDing et al. [27] are given in Table 4. Mechanical tests for $\text{Al}_{65}\text{Cu}_{20}\text{Fe}_{15}$ intermetallic alloy show a hardness in the range of 10-14 GPa. Alloy hardness was measured after sputtering at 9.44 GPa. While the hardness of the coating after annealing for one hour at 550 °C to 13.49 GPa, which is 43% higher than the coating without heat treatment. Also, the hardness of the coating deposited on stainless steel after annealing for 2 hours at 750 °C to 14.75 GPa was achieved.

4.3.2. Physical Vapor Deposition

Physical vapor deposition (PVD) is a conventional method for depositing various materials from the vapor phase that can physically produce thin layers or coatings on the surface of various substrates. These vapors of metals or alloys are in ionic, electron, or neutral forms. The main stages of the PVD from the vapor phase under vacuum conditions include evaporation of the source material, transfer of steam from the source to the substrate, and formation of a thin layer on the substrate with the accumulation of vapor from the source material. In this method, it is possible to adjust the thickness of the saturated coating by controlling the amount of

accumulated material. The PVD is an environmentally friendly process and allows the production of coatings with uniform thickness and suitable hardness. The suitable vacuum for the successful performance of this method is in the pressure range of 10^{-9} - 10^{-12} Torr and a combination of mechanical pumps and turbo is used to achieve it [30].

The Advantages of the PVD methods are [30, 31]:

- PVD coatings are sometimes harder and more resistant than coatings coated by the plating process. Most coatings have a high temperature and good strength, excellent wear resistance and are so durable that protective coatings are rarely necessary.
- The ability to use virtually any type of minerals and some organic coatings in a group of infrastructure and surfaces alike.
- Eco-friendly to traditional coating processes such as plating and painting.
- More than one technique can be used to place a specific film.
- Materials with improved properties (for example, better mechanical properties, etc.) can be deposited on another material.

The Disadvantages of the PVD methods are [30, 31]:

- Specific technologies can impose limitations.
- Some PVD techniques typically operate at very high temperatures and reactions and require special attention by operating personnel.
- There is a need for a cold water system to discharge large heat loads.
- The rate of sedimentation rate is usually low.
- Need for expensive equipment.

Daniels et al [30]. in the study of fabrication of Al-Cu-Fe-Cr and Al-Cu-Fe quasicrystalline phases by PVD method, sputtering targets with vacuum

powder mixture at 400 °C and orthorhombic and rhombohedral phases by sputtering method. Targets Al-Cu-Fe and Anil were obtained at 850 and 450 °C. One of the most recent published articles on Al-Cu-Fe ternary compounds is the research of Parsamehr et al [31], in Taiwan and the United States by applying coating by the sputtering method. They divided the dynamic growth mechanism of Al-Cu-Fe quasicrystal into two stages. In the first stage at low temperatures of about 200 to 350 °C, copper and aluminum were mixed and cavities were observed in their joint. With increasing temperature, aluminum and copper reacted together and mostly e-Al₂Cu phase was obtained. In the second stage, the temperature was increased to about 470 °C, which resulted in a triple-phase with higher stability. Finally, after increasing the temperature to 800 °C and achieving stable thermodynamic phases, the samples were cooled to room temperature. In this process, the cooling of quasi-crystalline phases was observed specifically at 660 °C.

4.3.3. Thermal spraying

Thermal spraying processes are processes in which fine or semi-molten droplets are sprayed onto the surface to form a coating. The raw material can be in the form of wire or powder and its material can be ceramic, metal, alloy, polymer or composite. Meanwhile, the method High Velocity Oxygen Fuel (HVOF) due to high heat application and very high speed, can create coatings with very good quality in terms of physical, mechanical, and chemical properties. For example, in terms of mechanical properties, very hard coatings (900 HV1000) are obtained in this way, but in return, there are limitations in terms of toughness [32].

Coverage in this technique is done using a combination of thermal energy and kinetic energy. Plasma spraying is the most common method of spraying thermal coating. In this process, the material to be inserted enters the plasma jet and

exits a plasma torch. This method is often used to create coatings on structural materials. These coatings are highly resistant to high temperatures, corrosion, and erosion. Vacuum plasma spray technology has the advantage of reducing the oxidation of the powder and the coated layer, thus providing a more controllable coating with greater uniformity and fewer impurities. HVOF has been used to improve surface properties such as increasing hardness, reducing friction, and increasing wear resistance. Al-Cu-Fe-Cr coating was applied to the titanium substrate by low pressure plasma spray (LPPS). The coating was applied evenly on the substrate and no cracks or separations were created on the surface. At temperatures of 750 and 800 °C, the oxidation resistance of the coating and substrate was investigated. Figure 7 shows the weight gain of the coating and the substrate under oxidation conditions over time [32]. It is seen that applying of Al-Cu-Fe-Cr coating considerably improved the oxidation resistance of the substrate.

In the formation of Al-Cu-Fe-Cr coating on the steel substrate by HVOF method, the hardness of this coating was about 485 HV0.05 [33, 34].

Comparison of formed phases, percentage of porosity, and microhardness of Al-Cu-Fe-Cr-B and Al-Ni-Co-Si coatings by plasma and HVOF methods are mentioned in Table 5. Stable values of the coefficient of friction depend on the method of coating application. Harder Al-Cu-Fe-Cr-B coatings have a lower coefficient of friction and better wear resistance. Also, the best application of Al-Ni-Co-Si coating was obtained by HVOF method [35].

In the HVOF method, Al-Cu-Fe coating with a thickness of 100 microns was obtained. The thermal spray method has advantages over the methods of physical vapor deposition and laser coating. For example, these two methods have very high operating costs and are also not suitable for physical vapor deposition methods for thicknesses higher than 10 micrometers [36].

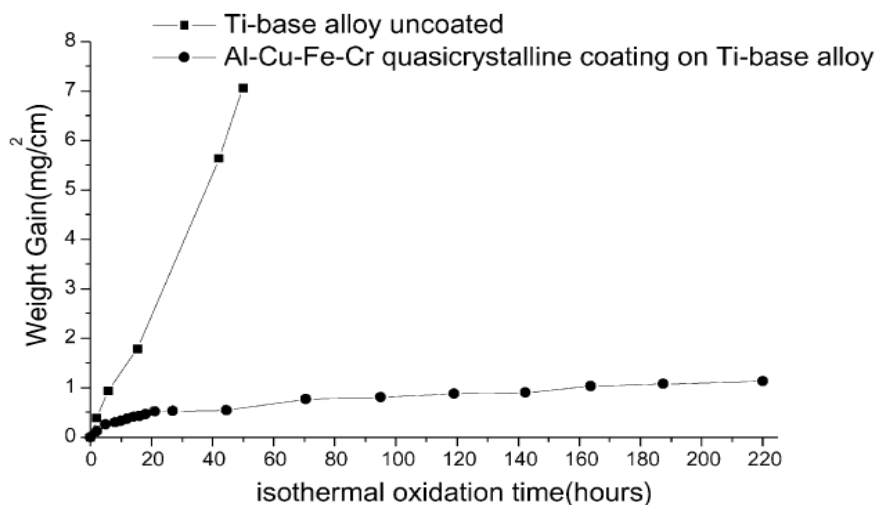


Fig. 7. Weight loss of the coating and the substrate under oxidation conditions over time [33].

Table 5. Composition phase constituents, porosity level and microhardness of the quasicrystalline coatings [35].

Coatings and counter materials		Phase constituents	Polarity level (%)	Vickers microhardness (kg/mm ²)
Al–Cu–Fe–Cr–B	Plasma HVOF	d+i+a+ λ + β	12.6 \pm 2.1	584 \pm 43
		d+i+a+ λ + β	6.9 \pm 1.8	605 \pm 34
Al–Ni–Co–Si	Plasma HVOF	d+ γ	11.8 \pm 1.8	559 \pm 46
		d+ γ	6.3 \pm 1.1	577 \pm 50
Cr	Electroplating	-	-	1003 \pm 33

Table 6. Comparison of the different fabrication process characteristics of quasicrystals [45].

	Melting and solidification	Melt spinning	Gas atomization	Mechanical alloying
Suitable for quasicrystals of thermodynamical stability	Stable	Metastable	Metastable	Metastable
Phase structure of quasicrystalline products	Single-phase Structure generally achieved by successive heat treatment	Single-phase Structure achievable both directly and by successive heat treatment	Single-phase Structure achievable both directly and by successive heat treatment	Single-phase Structure achievable both directly and by successive heat treatment
The shape of quasicrystalline products	Desired	Thin ribbon	Powder with a grain size smaller than 150 μ m	A fine powder with a layered structure
Quality of produced quasicrystals	High, sharp X-ray diffraction peaks, pores may exist in the structure if crystalline phases coexist	Broadening of X-ray peaks may occur; phasons	Generally high, sharp X-ray diffraction peaks	Broadening of X-ray peaks may occur, may occur, phasons; the ordering of the face-centered structure may not be complete
Contamination resources	Air	Air	Air	Air, grinding media, grinding vessel
Further processing possibilities	Heat treatment	Compaction, grinding and compaction, (heat treatment; quasicrystalline phases may decompose during annealing)	Thermal spraying, compaction, sintering, mechanical alloying, (heat treatment)	Compaction, thermal spraying, (heat treatment)

Coatings made by thermal spray method due to the rapid cooling of high internal stress on the coating and substrate, thus leading to cracks. The coating prepared by the HVOF method has less porosity than other thermal spray methods. Conditions that affect the hardness, friction coefficient, and wear resistance of coatings. Another disadvantage of the thermal spraying method is that during the spraying the powder will undergo phase changes and will be partially oxidized. Therefore, the coverage will

include other phases. Cold spraying is used for plastic metal coatings, which will be free of the above problems [37-38]. Other research has been done to fabricate the Al-Cu-Fe pseudocrystal at 570 to 890 Kelvin. Using the measured values of fracture toughness and thermal expansion coefficient, the critical thickness of Al-Cu-Fe coating deposited in the temperature range of 520-920 K on the substrate with different thermal expansion coefficients was calculated. Fig. 8. shows

that as the deposition temperature increases, the critical thickness of the coating decreases. [39-40].

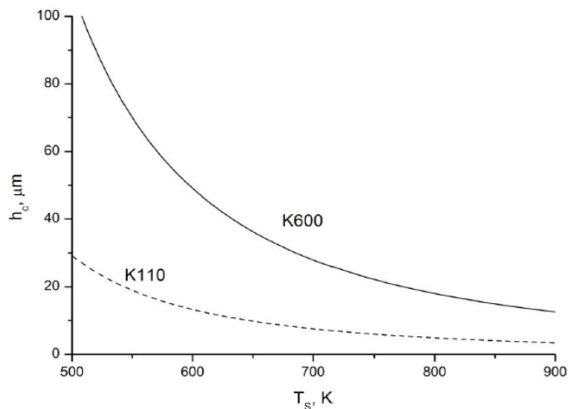


Fig. 8. Dependence of critical thickness for Al-Cu-Fe deposited onto substrates with expansion coefficient of $a_c = 12.1 \times 10^{-6} \text{ K}^{-1}$ (steel K100) and $a_c = 14.5 \times 10^{-6} \text{ K}^{-1}$ (steel K600) on the deposition temperature [41].

Finally, a set of common methods used to produce these materials and their related properties is shown in Table. 6. Depending on the type of structure, stable or quasi-stable quasicrystal, the type of need for heat treatment and other items that are compared in the Table. 6., the optimal production method can be selected. It should be noted that there are other methods such as laser cladding and electrodeposited to achieve the quasi-crystalline phase, but have been more limited studies [42-45].

5. Conclusion

Quasicrystals are new materials that can be used in many fields of technology. In this paper, common manufacturing methods and their related properties were investigated from the position of a materials engineer. As a result, the emphasis was placed on describing the fundamental differences between the methods of producing quasi-crystalline materials for structure and properties.

Quasicrystals are attractive materials: crystal structures, with their five-fold symmetry, are unfamiliar and their properties are surprising and could be very useful. Of course, it is clear that there are still many problems, such as the industrial production of quasicrystal with high quantity and quality that we must study and research. The cost of materials and traditionalism in industries must also be considered. But the research is promising and effective.

Quasicrystals are new materials that can be used in many fields of technology. In this paper, common manufacturing methods and their related properties were investigated from the position of a materials engineer. As a result, the emphasis was placed on describing the fundamental differences between the methods of producing quasi-crystalline materials for structure and properties.

From the studies performed, it can be concluded that the production of composites by melt spinning is a common and effective method. The mechanical alloying method is very suitable due to its speed at low temperatures. Creating a controllable coating with high uniformity and fewer impurities is possible using plasma spray technology in a vacuum.

Methods of physical vapor deposition and laser coating have very high operating costs and also the vapor deposition method is not suitable for thicknesses higher than 10 micrometers.

Coatings made by heat spray method cause cracks due to rapid cooling. Also, the coating prepared by the HVOF method has less porosity than other thermal spray methods.

References

- [1] D. Shechtman, I. Blech, D. Gratias, and J.W. Cahn, *Phys. Rev. Lett.*, 53(1984), 1951.
- [2] T.A. Corcovilos, and J. Mittal, *Appl. Opt.*, 58(2019), 2256.
- [3] M. Gogebakan, and B. Avar, *Mater. Sci. Technol.*, 26(2010), 920.
- [4] E. Karakose, and M. Keskin, *Met. Mater. Int.*, 18(2012), 257.
- [5] N. Fujita, H. Takano, A. Yamamoto, and A. P. Tsai, *Acta Crystallogr. Sect. A*, 69(2013), 322.
- [6] M. Mihalkovic, J. Richmond-Decker, C. Henley, and M. Oxborrow, *Philos. Mag.*, 94(2014), 1529.
- [7] M. Mihalkovic, and M. Widom, *Phys. Rev. res.*, 2(2020), 1.
- [8] A. P. Tsai, *Acc. Chem. Res.*, 36(2003), 31.
- [9] M. M. Rueda, M. C. Auscher, R. Fulchiron, T. Perie, G. Martin, and P. Sonntag, *Prog Polym Sci.*, 66(2017), 22.
- [10] J. Sladek, V. Sladek, and S. N. Atluri, *Eng Fract Mech.*, 140(2015), 61.
- [11] T. P. Yadav and N. K. Mukhopadhyay, *Curr. Opin. Chem. Eng.*, 19(2018), 163.
- [16] W. Wolf, C. Bolfarini, C. S. Kiminami, and W. J. Botta, *J. Alloys Compd.*, 823(2020), 153765.
- [17] R. Babilas, K. Młynarek, W. Łoński, D. Łukowiec, M. Kądziółka-Gaweł, T. Czeppe, and L. Temleitner, *Mater.*, 14(2021), 54.
- [18] Z. Chen, Y. Hou, B. Xie and Qi Zhang, *Mater.*, 13(2020), 2388.
- [19] A. Školáková, P. Novák, L. Mejzlíková, F. Pruša, P. Salvetr and D. Vojtech, *Mater.*, 10(2017), 1269.
- [20] K. Stan, L. L. Dobrzyńska, J. D. Ł. Rogal, and A. M. Janus, *Solid State Phenom.*, 186(2012), 255.
- [21] F. Zupanic, T. Boncina, A. Krizman, W. Grogger, C. Gspan, B. Markoli, and S. Spaic, *J. Alloys Compd.*, 452(2008), 343.
- [22] M. Amini, M. R. Rahimpour, S. A. Tayebifard, and Y. Palizdar, *Adv Powder Technol.*, 31(2020), 4319.

- [23] M. Amini, M. R. Rahimipour, S. A. Tayebifard, and Y. Palizdar, *Mater. Res. Express.*, 7(2020), 06501.
- [24] R. Ali, M. U. Akhtar, A. Zahoor, F. Ali, S. Scudino, R. N. Shahid, N. U. Haq Tariq, V. C. Srivastava, and V. Uhlenwinkel, *Mater. Chem. Phys.*, 251(2020), 123071.
- [25] D. N. Travessa, K. R. Cardoso, W. Wolf, A. M. Jorge Junior, and W. J. Botta, *Mater. Res.*, 15(2012), 749.
- [26] V. Brien, A. Dauscher, and F. Machizaud, *J. Appl. Phys. A*, 100(2006), 43503.
- [27] Y. Ding, D. O. Northwood, A. T. Alpas, *Surf. Coat. Technol.*, 96(1997), 140 .
- [28] Y. Liu, J. Padmanabhan, and B. Cheung, *Sci. Rep.*, (2016), 1.
- [29] W. Wolf, A. S. Kube, S. Sohn, Y. Xie, J. J. Cha, B. E. Scanley, C. S. Kiminami, C. Bolfarini, W. J. Botta and J. Schroers, *Sci. Rep.*, 9(2019).
- [30] M. J. Daniels, D. King, L. Fehrenbacher, J. S. Zabinski, and J. C. Bilello, *Surf. Coat. Technol.*, 191(2005), 96.
- [31] H. Parsamehr, T. Chen, D. Wang, M. Leu, I.Han , Z. Xi , A. Tsai , A. J. Shahani, and C. Lai , *Mate.*, 8(2019) ,100432.
- [32] J. Mora, P. GarcÁa, R. Muelas, and A. Agero, *Coat.*, 10(2020), 290.
- [33] J. Kong, C. Zhou, S. Gong, and H. Xu, *Surf. Coat. Technol.*, 165(2003), 281.
- [34] E. H. Saarivirta, E. Turunen, and M. Kallio, , *J. Alloys Compd.*, 354(2003), 269.
- [35] E. Fleury, Y. Ckim, J. Skim, D. Hkim, W. Tkim, H. Sahn, and S. M. Lee, , *J. Alloys Compd.*, 342(2002), 321.
- [36] H. Parsamehr, C. L. Yang, W. T. Liu, S. W. Chen, S. Y. Chang, L.J. Chen, A. P. Tsai, and C. H. Lai, *Acta Mater.*, 174(2019), 1.
- [37] H. Parsamehr, Y. J. Lu, T. Y. Lin, A. P. tsai and C.H. Lai, *Sci. Rep.*, 9(2019), 10.
- [38] W. Wolf, C. Bolfarini, C. S. Kiminami, and W. J. Botta, *J. Alloys Compd.*, 823(2020), 153765.
- [39] A. A. Lapeshev , O. A. Bayukov , E. A. Rozhkova , I. V. Karpov , A. V. Ushakov , and L. Y. Fe- dorov, *Phys. Solid State.*, 57(2015), 255.
- [40] A. A. Lapeshev , E. A. Rozhkova , I. V. Karpov , A. V. Ushakov , and L. Y. Fedorov , *Phys. Solid State.*, 55(2013) 2531.
- [41] S. Polishchuk , A. Ustinov , V. Telychko , A. Merstallinger , G. Mozdzen , and T. Mel- nichenko , *Surf. Coat. Technol.*, 291(2016), 406.
- [42] K. Biswas , R. Galun , B.L. Mordike ,and K. Chattopadhyay , *J. Non Cryst. Solids.*, 334(2004), 517.
- [43] Z. Minevski , C. L. Tennakoon , and K. C. Anderson , *Mater. Res. Soc.*, 805(2004).
- [44] K. Nan, F. Yingqing, C. Pierre, G. Bruno, L. Hanlin, and C. Christian, *Mater. Des.*, 132(2017), 105.
- [45] E. H. Saarivirta, *J. Alloy. Compd.*, 363(2004), 150.